

---

## Functional characterization of microRNA-27a-3p expression in human polycystic ovary syndrome

Mingming Wang, Jing Sun, Bo Xu, Marcin Chrusciel, Jun Gao, Maciei Bazert, Joanna Stelmaszewska, Yunyun Xu, Hongwen Zhang, Leszek Pawelczyk, Fei Sun, Nafis Rahman, Sławomir Wołczyński, Suk Ying Tsang, Xiangdong Li

*Endocrinology*  
Endocrine Society

Submitted: March 01, 2017

Accepted: September 14, 2017

First Online: September 29, 2017

---

Advance Articles are PDF versions of manuscripts that have been peer reviewed and accepted but not yet copyedited. The manuscripts are published online as soon as possible after acceptance and before the copyedited, typeset articles are published. They are posted "as is" (i.e., as submitted by the authors at the modification stage), and do not reflect editorial changes. No corrections/changes to the PDF manuscripts are accepted. Accordingly, there likely will be differences between the Advance Article manuscripts and the final, typeset articles. The manuscripts remain listed on the Advance Article page until the final, typeset articles are posted. At that point, the manuscripts are removed from the Advance Article page.

---

DISCLAIMER: These manuscripts are provided "as is" without warranty of any kind, either express or particular purpose, or non-infringement. Changes will be made to these manuscripts before publication. Review and/or use or reliance on these materials is at the discretion and risk of the reader/user. In no event shall the Endocrine Society be liable for damages of any kind arising references to, products or publications do not imply endorsement of that product or publication.

Functional roles of miR-27a-3p in human PCOS

## Functional characterization of microRNA-27a-3p expression in human polycystic ovary syndrome

Mingming Wang<sup>1</sup>, Jing Sun<sup>1</sup>, Bo Xu<sup>2</sup>, Marcin Chrusciel<sup>3</sup>, Jun Gao<sup>1</sup>, Maciei Bazert<sup>4</sup>, Joanna Stelmaszewska<sup>5</sup>, Yunyun Xu<sup>6</sup>, Hongwen Zhang<sup>7</sup>, Leszek Pawelczyk<sup>4</sup>, Fei Sun<sup>8</sup>, Nafis Rahman<sup>3,5</sup>, Sławomir Wołczyński<sup>5</sup>, Suk Ying Tsang<sup>9</sup>, Xiangdong Li<sup>1, #</sup>

<sup>1</sup>State Key Laboratory of Agrobiotechnology, College of Biological Sciences, China Agricultural University, Beijing 100193, China.

<sup>2</sup>Center for Reproductive Medicine, Anhui Provincial Hospital Affiliated to Anhui Medical University, Hefei, Anhui 230001, China.

<sup>3</sup>Institute of Biomedicine, Department of Physiology, University of Turku, Turku 20520, Finland.

<sup>4</sup>Department of Infertility and Reproductive Endocrinology, Poznan University of Medical Sciences, 60535 Poznan, Poland.

<sup>5</sup>Department of Reproduction and Gynecological Endocrinology, Medical University of Bialystok, Bialystok 15276, Poland.

<sup>6</sup>Department of General Medicine, First Affiliated Hospital of Kunming Medical University, Kunming, Yunnan 650032, China.

<sup>7</sup>Department of General Surgery, 306th Hospital of PLA, Beijing 100101, China.

<sup>8</sup>School of Life Sciences, University of Science and Technology of China, Hefei, Anhui 230026, China.

<sup>9</sup>School of Life Science and State Key Laboratory of Agro-Biotechnology, Chinese University of Hong Kong, Hong Kong, 999077, China.

Received 01 March 2017. Accepted 14 September 2017.

### Abbreviations :

miR-27a-3p, microRNA-27a-3p; miR-NC, miRNA negative control; E<sub>2</sub>, estradiol; GCs, granulosa cells; P<sub>4</sub>, progesterone; PI, propidium iodide; qPCR, real-time quantitative PCR; GAPDH, glyceraldehyde 3-phosphate dehydrogenase; PCNA proliferating cell nuclear antigen; PCOS, polycystic ovary syndrome; SMAD5, sterile alpha motif domain containing; 3'UTR, 3' untranslated regions; STAT1, signal transducer and activator of transcription 1; STAT3, signal transducer and activator of transcription 3.

The goal of this study was to characterize the function of microRNA-27a-3p (miR-27a-3p) in polycystic ovary syndrome (PCOS). MiR-27a-3p expression was analyzed in excised granulosa cells (GCs) from 21 PCOS and 12 normal patients undergoing IVF cycle treatments, and in 17 non-treated cuneiform ovarian resection PCOS **samples** and 13 control ovarian samples-**from** non-PCOS patients. We found **that** the expression of miR-27a-3p was significantly **increased** in

both excised GCs and the ovaries of PCOS patients compared to the controls. Insulin treatment of the human granulosa-like tumor cell line KGN resulted in decreased downregulated the expression of miR-27a-3p, and this effect appeared to be mediated by STAT1 and STAT3. The overexpression of miR-27a-3p in KGN cells inhibited SMAD5, which in turn decreased cell proliferation and promoted cell apoptosis. After KGN cells were stimulated with insulin for 48 h, there was increased expression of SMAD5 protein and decreased apoptosis. Additionally, knockdown/overexpression of SMAD5 in KGN cells reduced/increased cell number and promoted/ inhibited cell apoptosis. Insulin-stimulated primary GCs isolated from PCOS patients, in contrast to normal GCs or KGN cells, did not exhibit decreased miR-27a-3p expression. The differences in the expression levels in KGN cells and human PCOS GCs are likely explained by increased miR-27a-3p expression in the GCs caused by insulin resistance in PCOS. Taken together, our data provided evidence for a functional role of miR-27a-3p in the GCs dysfunction that occurs in human PCOS patients.

A functional role was identified for the upregulated miR-27a-3p expression in the observed granulosa cell dysfunction in human PCOS patients.

## INTRODUCTION

Polycystic ovary syndrome (PCOS) is one of the most common endocrine and metabolic disorders in women of reproductive age, and is characterized by hyperandrogenemia with arrest of follicle growth and ovulatory dysfunction (1-3). It has been reported that 75 % of infertile women may suffer from PCOS worldwide (4). The majority of PCOS patients exhibit insulin resistance (IR), leading to hyperinsulinemia and increased risk for type 2 diabetes mellitus and cardiovascular disease (5). PCOS patients often have elevated levels of ovarian androgens, and about 50 % of patients show elevated serum dehydroepiandrosterone sulfate (DHEAS), potentially of adrenal origin (6). Several genetic and environmental factors have been reported to contribute to the development of PCOS (2,7). However, the underlying molecular mechanism leading to PCOS remains unclear.

Granulosa cells (GCs) play an important role during folliculogenesis. Proliferating GCs provide a suitable microenvironment for follicle growth initiation, oocyte maturation, and atresia (8). Dysfunction of GCs in PCOS patients including decreased proliferation, increased apoptosis, or unbalanced hormone production may contribute to abnormal folliculogenesis (9,10).

MicroRNAs (miRNAs) are 21-25-nucleotide non-coding RNAs that are able to post-transcriptionally regulate gene expression (11). These miRNAs function as important regulators of various physiological and pathological processes, such as development, cell proliferation, differentiation, migration, and apoptosis (12-14). It has been suggested that ovarian miRNAs may play a role in PCOS (15,16). McCallie et al. showed that the expression levels of 6 miRNAs including hsa-let-7a, hsa-miR-19a, hsa-miR-19b, hsa-miR-24, hsa-miR-92, and hsa-miR-93, were noticeably downregulated in PCOS blastocysts compared to controls (17). Similarly, Roth et al. reported decreased expression of miR-132 and miR-320 in the follicular fluid of PCOS

patients (18). In addition, several serum miRNAs differentially expressed in PCOS patients were suggested to play key roles in pathological insulin signaling, inflammation, and hormone secretion (15). Although the abnormal expression of miRNAs directly **affects follicular** development and the normal physiological function of ovaries, the role of miRNAs in PCOS GCs remains unknown.

Our recent profiling data analysis **predicted** that novel miRNAs may be involved in the pathophysiology of PCOS (3). The recent advancements in high-throughput profiling and sequencing provide a comprehensive tool to understand the various signaling pathways and molecular networks involved in the etiology and pathophysiology of PCOS. Thus, **our next goal was** to dissect the functional role of individual miRNA participating in the pathology. In this study, we focused on the functional characterization of miR-27a-3p expression in ovaries and GCs from PCOS patients. **Additionally, we analyzed miR-27a-3p function** using a human granulosa tumor-like cell line to explore the mechanistic role of miR-27a-3p in the dysfunction of GCs.

## MATERIALS AND METHODS

### *Human granulosa cells (GCs)*

We analyzed GCs excised from a total of 42 donor patients [healthy control patients, n=17 (qPCR analysis, n=13; *in vitro* n=4) and PCOS patients, n=25 (qPCR analysis, n=21; *in vitro* n=4)] undergoing in vitro fertilization (IVF) stimulation cycles with the classical standard protocol of GnRH antagonist (Cetrotide) 0.25 mg subcutaneously. (s.c.) + recombinant FSH 150 IU s.c. + ovulation peak induced by 0.2 mg (Gonapeptyl) daily ferring s.c. GnRH agonist (19). **The revised criteria from the Rotterdam European Society of Human Reproduction (ESHRE) and Embryology/American Society (ASRM) (17,20) were used for diagnosis of PCOS.** GCs were obtained by follicular fluid aspiration. After oocyte removal, follicular fluid containing GCs were pooled and centrifuged at 250 x g for 10 min. The fraction **containing the** GCs was carefully aspirated, transferred to a new centrifuge tube, resuspended, washed in PBS (Gibco, USA), and then centrifuged at 250 x g for 5 min. GC pellets were lysed with TRIsure (Bioline, UK) for total RNA extraction or resuspended in culture medium for *in vitro* studies. Only GCs from follicles with mature oocytes (MII) were included in this study. The local Human Investigation Ethics Committee at the Medical University of Bialystok, Bialystok, Poland approved the study (license number R -I - 002 /146/2016). Written informed consent was obtained from all patients/donors before the study.

### *Human ovarian samples*

We examined ovaries from a total number of 30 patients (normal healthy control patients, n=13 and PCOS patients, n=17). This study group included patients of reproductive age, with PCOS diagnosed according to the ESHRE and ASRM criteria (20). The PCOS patients qualified for an ovarian cuneiform resection by laparoscopy due to a lack of ovarian response to multiple (3-6) cycles of clomiphene citrate stimulation or treatment with pituitary gonadotropin hormones. The

control ovarian group (n=13) consisted of patients of reproductive age who did not meet the PCOS diagnostic criteria (20) but who had undergone surgical procedures for other reasons, such as small ovarian cysts, fibroids, chronic pelvic pain, or for diagnostic infertility laparoscopy that may have required a biopsy of healthy tissues or lesion removal with a healthy tissue margin. The patient exclusion criteria for both groups were as follows: ovarian, adrenal, endometrial, cervical and breast neoplasms, pelvic endometriosis, congenital adrenal hyperplasia, clinically and/or laboratory-confirmed endocrine disease (thyroid dysfunction, acromegaly, gigantism, or Cushing's disease), diabetes type I or II, hyperprolactinemia, and unexplained vaginal bleeding. Ovarian coneiform resection samples were collected during laparoscopic surgery, protected against RNA degradation by mixing with RNA later (Life Technologies, USA), snap-frozen in liquid nitrogen, and stored at -80 °C until analyzed. The local Human Investigation Ethics Committee at the Medical University of Poznan, Poznan, Poland approved the study (license number 955/16). Written informed consent was obtained from all patients/donors before the study.

#### **Total RNA isolation**

Total RNA was isolated from human ovaries and GCs using a Trizol-based standard extraction protocol according to the manufacturer's instructions (Life Technologies, USA). The total RNA concentration was quantified using a NanoDrop 1000 spectrophotometer (NanoDrop Technologies, USA).

#### **Reverse transcription (RT) and real-time quantitative PCR (qPCR)**

For normal and PCOS ovarian/GCs total RNA samples, RT was performed with the SensiFAST™ cDNA Synthesis Kit (Bioline, UK). Prior to cDNA synthesis, 1 µg of total RNA was incubated with 1 µl of DNase I according to the manufacturer's protocol (Invitrogen, USA). RT was performed in a thermal cycler using the following conditions: 25 °C - 10 min, 42 °C - 15 min, 48 °C - 15 min (an additional step for highly-structured RNA), 85 °C - 5 min, and then 4 °C. Next, qPCR was performed with DyNAmo HS SYBR Green qPCR Kit (Thermo Fisher Scientific, USA) and the primers indicated in Table 3 using the CFX96 Touch™ Real-Time PCR Detection System (Bio-Rad, USA). Following an initial denaturation at 95 °C for 10 min, 40 cycles of PCR amplification were performed of 95 °C for 10 s, 58-60 °C for 20 s, and 72 °C for 15 s.

For KGN and Hela cells, RT was performed with the cDNA Synthesis Kit (Thermo Scientific, USA) using the following conditions: 42°C-90 min, 95 °C - 5 min, followed by a hold at 4 °C. Next, cDNA was amplified in a Roche LightCycler 480 system (Roche, Switzerland), using SYBR Green Master Mix Reagent (Roche, Switzerland). Cycling conditions were as follows: denaturation for 10 min at 95 °C followed by 40 cycles of 10 s at 95 °C, 10 s at 60 °C, and 10 s at 72 °C.

The specificity of qPCR amplification was verified by performing a melting curve analysis and agarose gel electrophoresis. Relative gene expression was calculated by the efficiency-corrected  $\Delta\Delta C_t$  method, normalized to the index (geometric mean) of four housekeeping genes:



cyclophilin A (PPIA),  $\beta$ -actin (ACTB),  $\beta$ -glucuronidase (GUSB), and glyceraldehyde 3-phosphate dehydrogenase (GAPDH). Each sample in every group was measured in duplicate.

#### ***RT and qPCR to measure miRNA expression***

RT was performed with the TaqMan® MicroRNA Reverse Transcription Kit (Thermo Fisher Scientific, USA) according to the manufacturer's protocol in a thermal cycler using the following conditions: 16 °C - 30 min, 42 °C - 30 min, 85 °C - 5 min, and then 4 °C. The miRNA primers/probes used in this study were purchased commercially (Thermo Fisher Scientific, USA) and are shown in Supplemental Table 3. For the PCOS samples, qPCR was performed with TaqMan® Universal Master Mix II (Thermo Fisher Scientific, USA) using the CFX96 Touch™ Real-Time PCR Detection System (Bio-Rad, USA). Following an initial denaturation at 95 °C for 10 min, 40 cycles of PCR amplification were performed at 95 °C for 15 s and 60 °C for 1 min. For KGN and HeLa cells, qPCR was performed in a Roche LightCycler 480 system (Roche, Switzerland), using SYBR Green Master Mix Reagent (Roche, Switzerland) with the following conditions: denaturation for 10 min at 95 °C followed by 40 cycles of 10 s at 95 °C, 10 s at 60 °C, and 10 s at 72 °C. Relative miRNA expression was calculated by the efficiency-corrected  $\Delta\Delta C_t$  method, and was normalized to the endogenous control U6 snRNA. Each sample in every group was measured in duplicate.

#### ***Cell culture***

For *in vitro* studies, we used human primary GCs from PCOS and normal healthy female patents, as well as a steroidogenic human granulosa-like tumor cell line KGN (21). GCs were obtained from woman with PCOS (n=4) and healthy controls (n=4) undergoing *in vitro* fertilization treatment. After oocyte removal, **samples of** follicular fluid containing GCs were sedimented for 30 min. The fraction with GCs was carefully transferred to a new tube and resuspended in culture medium [DMEM/F12 medium (Sigma, USA) with 10 % FBS (Gibco, USA) and 1 % antibiotics (100 U/ mL penicillin and 100  $\mu$ g/mL streptomycin; Sigma, USA). KGN cells are undifferentiated and maintain the physiological characteristics of ovarian cells, **with normal** expression of **the** functional FSH receptor and CYP19A1 (21). KGN cells were grown in DMEM/ F12 (Sigma, USA) supplemented with 10 % fetal bovine serum (Gibco, USA) and 1% antibiotics (100 U/mL penicillin and 100  $\mu$ g/mL streptomycin; Sigma, USA), and cultured at 37°C under 5% CO<sub>2</sub>. HeLa cells (ATCC CCL-2) were grown in DMEM/ High glucose (Sigma, USA) supplemented with 10% fetal bovine serum (Gibco, USA), and grown under the same culture conditions described above.

Cells were equally distributed onto a 12- well plate. After 12 h of incubation with full medium, cells were rinsed with PBS (Gibco, USA) and serum-starved for 12 h [DMEM/F12 medium with 0.5 % charcoal-stripped FBS (Gibco, USA)]. Next, the medium was exchanged for fresh **medium** with stimulation of 100, 10, or 1 ng/ml insulin, and full medium was used as a positive control. Cells were treated for 24 h, rinsed with PBS and then collected with the TRI Reagent™ Solution (Thermo Scientific, USA).

KGN cells or primary GCs from PCOS/ normal healthy control patients were plated in 6-well plates at  $2 \times 10^5$  per well. After starving for 12 h, the cells were treated without (0) or with insulin (Sigma, USA) at concentrations of 1, 10, and 100 ng/mL for 24 h to test the expression of miR-27a-3p (for both primary GCs and KGN cells) or 48 h to test the protein expression level of SMAD5 (for KGN cells).

### **Plasmids**

To experimentally determine if miR-27a-3p targets *SMAD5*, both the wild-type (5'-acuuugaguacagauacugugag-3') and mutated (5'-acuuugaguacagauacgcaag-3') 3'-UTRs of the *SMAD5* gene were cloned into the psi-CHECK-2 dual luciferase reporter vector (Promega, USA) using Not I and XhoI restriction sites. To study the effect of STAT1 and STAT3 on the expression of miR-27a-3p, the coding sequence of the STAT1 gene was cloned into the eukaryotic expression plasmid pEGFP-C1. To assess the effect of SMAD5 overexpression on KGN cells, we cloned the coding sequence of *SMAD5* into the eukaryotic expression plasmid pCDNA3.1. All generated constructs were confirmed by sequencing.

### **Transient transfection and luciferase activity assay**

KGN and/or HeLa cells were transfected with miRNA mimics or a miRNA negative control (miR-NC) using Lipofectamine 3000 (Invitrogen, USA) following the manufacturer's protocol. miRNA mimics and miR-NC were chemically synthesized by Shanghai GenePharma (Shanghai, China). Briefly, the day before transfection, cells were plated with normal growth medium and were 70-80% confluent at the time of transfection. The time of the start of transfection was considered time 0.

For reporter assays, HeLa cells were transiently transfected with reporter constructs together with miRNA mimics and miR-NC. Cell extracts were prepared 48 h after transfection, and the ratio of Renilla/firefly luciferase was measured with the Dual-Luciferase Reporter Assay System (Promega, USA).

### **Cell proliferation**

Cell proliferation was measured with the Cell Counting Kit-8 (CCK-8, Beyotime Institute of Biotechnology, China). Cells were seeded into 96-well plates at  $1 \times 10^4$  cells per well and cultured in growth medium. After stimulation, 10  $\mu$ L of the CCK-8 solution was added to each well and then incubated for 2 h. The cell numbers were measured in a PowerWave HT Microplate Spectrophotometer (BioTek, USA) by measuring the absorbance at a wavelength of 450 nm (OD 450).

### **Hormone analysis**

The culture medium was collected and the estradiol ( $E_2$ ) and progesterone ( $P_4$ ) concentrations were measured. The measurements were performed by radioimmunoassay by the Institute of Beijing North Biotechnology. Both the inter- and intra- variation of the  $E_2$  and  $P_4$  assays were below 10 %.

### **Cell apoptosis analysis**

Cell apoptosis was analyzed by annexin V/ **propidium iodide (PI)** staining. After stimulation, cells were washed twice with ice-cold PBS solution and resuspended in 100  $\mu$ L of 1 $\times$  annexin binding buffer with 5  $\mu$ L of annexin V-FITC (AV) (Sigma, USA) and 10  $\mu$ L of PI (Sigma, USA). The cells were incubated for 15 min at room temperature in the dark, and were then subjected to flow cytometric analysis using FACSCalibur (Becton Dickinson, USA). The data were analyzed by Flowjo software.

#### ***Cell cycle analysis***

For cell cycle analysis, cells were harvested after treatment and then fixed in 70% ethanol at 4°C overnight, permeabilized, and stained with PI. After incubation for 15 min, 400  $\mu$ L 1 $\times$  of binding buffer was added per sample and the mixture was filtered through a 200-mesh nylon net prior to cell fluorescence measurement using FACSCalibur (Becton Dickinson, USA). Data were analyzed by Flowjo software.

#### ***Western blotting***

Cells were rinsed with ice-cold PBS and **then the** protein was extracted using the RIPA method. Protein samples were separated by SDS-PAGE and then transferred to a PVDF membrane as described previously (22). After washing, the membranes were incubated with antibodies. Finally, the films were scanned and quantified using ImageJ software. Antibodies used in this study are shown in Table S2.

#### ***Microarray data***

The expression of SMAD5 in PCOS GCs was mined from the public data set GSE34526 (<https://www.ncbi.nlm.nih.gov/geo/query/acc.cgi?acc=GSE34526>).

#### ***Statistical analysis***

The results are presented as the means  $\pm$  standard error of the mean (SEM). Statistical significance was assessed by the two-tailed Student's t test using the GraphPad Prism 5 software. A P-value < 0.05 was considered statistically significant.

## **RESULTS**

### ***Changes in miR-27a-3p expression in PCOS ovaries and GCs.***

Using data from the published database (3), of the 59 known miRNAs differentially expressed in PCOS vs. control GCs (fold change > 2 and  $p < 0.05$ ), 21 miRNAs were upregulated and 38 were downregulated in PCOS GCs. We found that the up-regulated miRNAs miR-27a-3p and miR-27a-5p correlated with increased serum testosterone (T) in GCs from PCOS (Supplemental Table 1 [Table S1]). To validate the miRNA microarray results, we performed real time quantitative real-time PCR (qPCR) analysis **on samples** from non-treated healthy controls (n=13) and PCOS patients (n=17). Interestingly, miR-27a-3p was significantly upregulated in both GCs and ovaries from PCOS patients, but no **statistically** significant changes were observed for miR-27a-5p (Figures 1A-D). MiR-27a-3p is located on chromosome 8 in mouse and chromosome 19 in human, and is proximal to two other miRNAs, miR-23a and miR-24-2. We also checked the expression of these



two miRNAs, but no significant changes in miR-24-2 and miR-23a expression were observed in PCOS GCs and ovaries compared to the **level of expression in the controls** (Figures 1E-H). The hormonal treatment in the IVF protocol used for both the control and PCOS patients from whom the GCs were excised likely contributed to the observed identical miRNA expression patterns of the non-treated PCOS and control ovary miRNAs (Figures 1A-H). The characteristics of the participants are presented in Table 1.

***Insulin induced the down-regulation of miR-27a-3p expression mediated by STAT1 and STAT3 in human granulosa-like tumor KGN cells.***

Hyperinsulinemia is one of the most common features of PCOS. We hypothesized that miR-27a-3p may be regulated by insulin. We performed qPCR using KGN cells (21) stimulated with insulin to assess the expression of miR-27a-3p. The qPCR results showed approximately 0.40-fold and 0.50-fold decreases in the levels of miR-27a-3p after 24 h treatment with 10 and 100 ng/mL insulin respectively (Figure 2A). To determine the underlying mechanism of how insulin led to the downregulation of miR-27a-3p, we analyzed the region of 2000 nucleotides upstream of miR-27a-3p using the JASPAR database. Among the **potential** binding transcription factors (TFs), two TFs (signal transducer and activator of transcription 1/3 [STAT1/3]) were selected **based on** their multiple conserved predicted binding sites and their known roles in proliferation and apoptosis (Figure 2B). To clarify the effects of the two TFs, STAT1 and STAT3, on the expression of miR-27a-3p, we transfected a STAT1-overexpression vector (pEGFP-STAT1) and a control vector, pEGFP into KGN cells. The qPCR results showed a significant decrease of miR-27a-3p in the STAT1-overexpressed cells compared with controls (Figure 2C). To explore whether these two TFs are regulated by insulin, we **measured** the protein levels in KGN cells treated with insulin for 48 h and found that STAT1 and STAT3 were obviously decreased in the insulin-treated cells, **and** that this effect was dose-independent (Figures 2D-F). These data demonstrated that miR-27a-3p could be regulated by insulin and that this effect may be mediated by STAT1 and STAT3.

***Overexpression of miR-27a-3p decreased GC proliferation and promoted apoptosis in KGN cells.***

In order to assess the functional role of miR-27a-3p in GCs, we transfected either miR-27a-3p mimics or miR-NC into the KGN cell line. The expression of miR-27a-3p in cells after transfection was measured by qPCR analysis. Transfection with miR-27a-3p mimics increased intracellular miR-27a-3p levels by approximately 1700-fold (Figure 3A). Recent studies have reported that differential expression of miRNAs is involved in hormone secretion and proliferation in GCs (23-25). Next, we studied the production of (17) estradiol (E<sub>2</sub>) and progesterone (P<sub>4</sub>) by KGN cells in response to the overexpression of miR-27a-3p. The overexpression of miR-27a-3p had no effect on E<sub>2</sub> and P<sub>4</sub> production in GCs (Supplementary Figure 1A [Figure S1A]). Using the CCK-8 assay, we observed a significantly reduced number of GCs 48 h after transfection of miR-27a-3p mimics into GCs ( $P < 0.05$ ) (Figure 3B). To further demonstrate how miR-27a-3p **affects** GCs growth, we examined the apoptotic rate and cell cycle in KGN. Using Annexin V-FITC and propidium iodide (PI) staining and flow cytometry 48 h

post-transfection, we observed that the overexpression of miR-27a-3p significantly increased the apoptotic rate of KGN cells ( $P < 0.05$ ) (Figures 3C, S1B). Using PI staining and flow cytometry analysis, we observed no changes in cell numbers of G0/G1 phase and G2/M phase (Figure 3D). Also, we found that the protein expression levels of PCNA and the mRNA expression level of cell cycle-related genes (CDK6, cyclin D1, and cyclin E) were not altered (Figures 3E and 3F). All of these data indicated that miR-27a-3p decreased the number of GCs by promoting cell apoptosis.

#### ***SMAD5 is a potential target of miR-27a-3p in KGN cells.***

To study the effects of miR-27a-3p on apoptotic target mRNAs, seed-sequence-based predictions were performed in miRDB and TargetScan. Among the candidate targets of miR-27a-3p, we found that the SMAD5 gene seemed an appropriate candidate, because it is involved in cell apoptosis (26). The 3'-UTR of SMAD5 mRNA contains an evolutionarily conserved miR-27a-3p putative binding site in vertebrates (Figure S1C). To determine whether SMAD5 is a true target of miR-27a-3p, we constructed dual luciferase reporter vectors containing the wild-type 3'-UTR of SMAD5, as well as a mutant form of the miR-27a-3p seed sites (Figure S1D). Hela cells were co-transfected with the reporter plasmids and miR-27a-3p mimics or miR-NC, and harvested 48 h after transfection and assayed for dual luciferase activity. As shown in Figure 3G, the luciferase activity from the wild-type SMAD5 3'-UTR was reduced by 40% in the presence of the miR-27a-3p mimics. However, the mutant form of the seeding site abolished the silencing effects of miR-27a-3p on SMAD5 3'-UTR reporter activity. These results indicated that miR-27a-3p suppresses SMAD5 expression by directly binding to its 3'-UTR.

To validate that the SMAD5 gene is a target of miR-27a-3p, KGN cells were transfected with miR-27a-3p mimics or miR-NC. Next, qPCR and Western blot analysis were performed and the results revealed that the expression of SMAD5 mRNA (Figure 3H) and protein (Figure 3I) in KGN cells was significantly lower in miR-27a-3p transfected KGN compared to the control cells. Thus, our results demonstrated that the SMAD5 gene is a miR-27a-3p target and that miR-27a-3p regulates SMAD5 gene expression both at the transcriptional level and the post-transcriptional level. Additionally, we measured SMAD5 mRNA expression in the PCOS GCs and ovarian samples, and observed that SMAD5 was significantly downregulated in the PCOS group (Figures 3J and 3K). Interestingly, the expression profiling of human miRNAs from the public database (27) showed a similar result (Figure 3L). Taken together, the SMAD5 gene seemed a likely potential target of miR-27a-3p.

#### ***Knockdown/overexpression of SMAD5 reduced/increased apoptosis in KGN cells.***

We knocked down SMAD5 expression by using siRNA (si-SMAD5). The expression of SMAD5 mRNA (Figure 4A) and protein (Figure 4B) was decreased in cells transfected with si-SMAD5 for 48 h compared to the expression levels of the controls. Next, we measured the production of E<sub>2</sub> and P<sub>4</sub> by KGN cells, and found that knockdown of SMAD5 had no effect on E<sub>2</sub> and P<sub>4</sub> production in KGN cells (Figures S2A and S2B). By using the CCK-8 assay, we observed a significantly reduced number of KGN cells 24 h after transfection with si-SMAD5 ( $P < 0.05$ )

(Figure 4C). Using Annexin V-FITC and PI staining and flow cytometry 48 h post-transfection, we observed that knockdown of SMAD5 significantly increased the apoptotic rate of KGN cells ( $P<0.05$ ) (Figures 4D and S2D). Using PI staining and flow cytometry analysis, we observed no changes in the cell numbers of G0/G1 and G2/M phases (Figure S2C). Conversely, when we overexpressed SMAD5 in KGN cells, we observed an increased cell number (Figures 4G and S2H) and reduced apoptosis rate (Figures 4H and S2I) but no obvious change in the cell cycle (Figure S2G) or the hormone secretion of  $E_2$  and  $P_4$  (Figures S2E and S2F) (Figures 4E and 4F). All of these data showed that SMAD5 knockdown decreased the number of KGN cells by promoting cell apoptosis, which is similar to the effects of miR-27a-3p overexpression.

#### ***Insulin induced the upregulation of SMAD5 protein level and reduced apoptosis in KGN cells***

We showed that miR-27a-3p was regulated by insulin and promoted apoptosis in KGN cells. There are several reports that insulin could promote KGN cell proliferation (28,29). Therefore, we next explored the proliferation and apoptotic effects of insulin on KGN cells. We applied an insulin concentration of 100 ng/mL for 48 h and observed a significantly increased number of GCs by CCK-8 assay ( $P<0.05$ ), (Figure 5A) and inhibited apoptosis in KGN cells (Figures 5B and S3A). Additionally, the expression of SMAD5 was increased after the insulin treatment (Figures 5C and 5D). These data further demonstrated that miR-27a-3p promoted apoptosis in KGN cells by targeting SMAD5.

#### ***Insulin treatment of GCs derived from PCOS and normal patients***

GCs from PCOS and normal healthy patients were stimulated with varying doses of insulin to assess the effects on the expression of miR-27a-3p. QPCR analysis showed no significant changes in the PCOS GCs after insulin treatment vs. non-treated PCOS GCs, but miR-27a-3p levels were higher compared to the GCs from normal healthy women (Figure 6).

## **DISCUSSION**

A growing number of studies suggest that miR-27a-3p plays important functions in various physiological and pathological processes (30-32). Zhou et al. found that miR-27a-3p targets BTG2 in gastric cancer, and plays a role as a growth-promoting and anti-apoptotic factor (33). Another study reported that miR-27a-3p can induce apoptosis in human prostate cancer cells (34). These pro- or anti-apoptotic properties of miR-27a-3p suggested that miR-27a-3p may play different functions in different physiological states and pathological conditions according to the environmental context. GC apoptosis can induce follicular atresia, which leads to oocyte maturation and follicular developmental disorder. A high rate of apoptosis in GCs can prevent the conversion of androgen to estrogen, causing local hormones changes within the follicle and disturbing normal follicular development (35,36). Our data showed that the level of miR-27a-3p was increased/ upregulated in GCs of PCOS patients and that overexpression of miR-27a-3p in KGN cells inhibited proliferation and promoted apoptosis.. Additionally, we identified SMAD5, previously reported to regulate cell apoptosis, as a potential target of miR-27a-3p (37,38). We investigated this by Western, luciferase reporter assay, and flow cytometry. Our

results suggest that miR-27a-3p **may** target SMAD5 to promote apoptosis in KGN cells, which may suggest a potential role in PCOS pathogenesis due to GC apoptosis.

An earlier report showed that miR-23a and miR-27a promote human granulosa cell apoptosis by targeting SMAD5 (26). However, our results differ **from those results** in several ways. Nie et al. found that miR-27a-3p is upregulated in patients with premature ovarian failure (POF), but PCOS patients were excluded from their analysis. In our study, we focused on PCOS patients. We found that miR-27a-3p was upregulated and SMAD5 was downregulated in PCOS GCs. In contrast to normal GCs or KGN cells, due to insulin resistance, the expression of miR-27a-3p in PCOS GCs was not affected by insulin. Normal GCs or KGN cells responded to insulin treatment with decreased expression of miR-27a-3p and increased expression of SMAD5, and both these changes decreased apoptosis. Our data also showed that insulin levels in KGN cells downregulated the expression of miR-27a-3p and that this down-regulation occurred *via* STAT1 and STAT3, which was not reported previously.

GCs are the main source of steroidogenesis, including production of E<sub>2</sub> and P<sub>4</sub>. Gonadal steroids play key roles in ovarian follicular development, oocyte maturation, and ovulation (39). Some miRNAs were recently reported to influence steroid hormone release by ovarian GCs (40,41). In the present study, we observed that miR-27a-3p overexpression in KGN cells had no significant effect on E<sub>2</sub> and P<sub>4</sub> secretion. Thus, miR-27a-3p may utilize a strategy other than hormone secretion to affect GC function.

It is well known that insulin plays a key role in the regulation of ovarian function, and stimulates the proliferation and hormone production of GCs (22,42). Several miRNAs have been reported to be regulated by insulin in PCOS (29). Jiang et al. reported that high concentrations of insulin induced the upregulation of miR-93, stimulated KGN cell proliferation, and reduced CDKN1A expression in PCOS (28). Xiang et al. observed that insulin treatment in KGN cells inhibited miR-483, and promoted IGF1 and cell proliferation (29). In this work, we found that insulin could downregulate the expression of miR-27a-3p and inhibit apoptosis in KGN cells. The mechanism explaining the changes mediated by insulin in apoptosis and the effects on the TFs upstream of miR-27a-3p, STAT1 and STAT3, require further study. Additionally, further clinical investigations of miRNA expression for a large group of PCOS patients are needed.

Hyperandrogenism is a key endocrine characteristic of PCOS patients (43). Androgens are mainly produced in adrenal glands and ovaries, but the hyperandrogenism of PCOS is closely related to the ovaries (44). Androgens via the androgen receptor (AR) **to induce** induced the expression of miR-125b in mouse GCs, KGN cells, and GCs from women undergoing in vitro fertilization (45). **Similarly,,**miR-27a-3p expression is regulated by androgen in prostate cancer, both transcriptionally and post-transcriptionally (46), Another study demonstrated activity of miR-27a-3p as an androgen-induced tumor suppressor, targeting MAP2K4 in prostate cancer (34). Although miR-27a-3p has been proposed to be an androgen-response miRNA, this analysis was not **within** the scope of **this** study.

Taken together, the first part of our study demonstrated significantly high levels of miR-27a-3p expression in PCOS GCs and ovary. The last part of the study showed the role of miR-27a-3p in the downregulation of SMAD5 and induction of apoptosis. However, there were contradictions between the findings in the first and last part of this study, as insulin downregulated microRNA-27a-3p expression in KGN cells, but samples from PCOS patients presented with higher levels of insulin and higher levels of miR-27a-3p expression. Thus the question is, if insulin decreased miR-27a-3p expression in GCs, how did the increased insulin level increase miR-27a-3p expression? Insulin-stimulated primary GCs isolated from PCOS patients, in contrast to normal GCs or human ovarian granulosa-like tumor cells (KGN cell line), did not respond to decreased miR-27a-3p expression. This lack of decreased miR-27a-3p expression in GCs of PCOS patients displaying increased insulin levels could be explained by the insulin resistance of GCs. In the regulation of miR-27a-3p expression, KGN cells exhibited characteristics of normal human GCs. Although the KGN cell line is a useful model to understand the regulation of steroidogenesis, cell growth, and apoptosis in human GCs (21), it might not be a good model to study GC functions in the context of insulin resistance or hyperinsulinemia.

#### Acknowledgments

We thank Prof. Toshihiko Yanase from Fukuoka University, Japan for the kind donation of the KGN cell line.

**Corresponding author:** Xiangdong Li, State Key Laboratory of Agrobiotechnology, College of Biological Sciences, China Agricultural University, Beijing 100193, China, Tel/Fax : 86-10-62734389, E-mail: [xiangdongli@cau.edu.cn](mailto:xiangdongli@cau.edu.cn)

This work was supported by grants from the National Science and Technology Major Project (2013ZX10004608), Natural Science Foundation of China (NSFC31071316 and NSFC81261130024), National Science and Technology Major Project (2012AA020601), Ministry of Science/Technology (2009CB941701), State Key Laboratory of Agrobiotechnology Grants (2015SKLAB6-13) and the CAU Scientific Fund (No. 2012YJ034).

#### Author contribution:

ST and XL designed the study concept; M.W, J.S, MC, J.G. and M.B performed the experiments; all the authors (MW, JS, BX, MC, JG, YX, MB, HZ, LP, FS, NR, SW, ST, XL) analyzed and interpreted the results; MW, MC, NR and XL drafted the manuscript and all the authors have approved the final manuscript.

#### Disclosure Statement:

I certify that neither I nor my co-authors have a conflict of interest that is relevant to the subject matter or materials included in this work.

#### References



1. Dasgupta S, Reddy BM. The Role of Epistasis in the Etiology of Polycystic Ovary Syndrome among Indian Women: SNP-SNP and SNP-Environment Interactions. *Ann Hum Genet* 2013; 77:288-298
2. Fux Otta C, Fiol de Cuneo M, Szafryk de Mereshian P. [Polycystic ovary syndrome: physiopathology review]. *Revista de la Facultad de Ciencias Medicas* 2013; 70:27-30
3. Xu B, Zhang YW, Tong XH, Liu YS. Characterization of microRNA profile in human cumulus granulosa cells: Identification of microRNAs that regulate Notch signaling and are associated with PCOS. *Molecular and cellular endocrinology* 2015; 404:26-36
4. Cankaya S, Demir B, Aksakal SE, Dilbaz B, Demirtas C, Goktolga U. Insulin resistance and its relationship with high molecular weight adiponectin in adolescents with polycystic ovary syndrome and a maternal history of polycystic ovary syndrome. *Fertil Steril* 2014; 102:826-830
5. Legro RS, Finegood D, Dunaif A. A fasting glucose to insulin ratio is a useful measure of insulin sensitivity in women with polycystic ovary syndrome. *The Journal of clinical endocrinology and metabolism* 1998; 83:2694-2698
6. Carmina E, Rosato F, Janni A. Increased DHEAs levels in PCO syndrome: evidence for the existence of two subgroups of patients. *Journal of endocrinological investigation* 1986; 9:5-9
7. Manneras-Holm L, Benrick A, Stener-Victorin E. Gene expression in subcutaneous adipose tissue differs in women with polycystic ovary syndrome and controls matched pair-wise for age, body weight, and body mass index. *Adipocyte* 2014; 3:190-196
8. Eppig JJ. Oocyte control of ovarian follicular development and function in mammals. *Reproduction* 2001; 122:829-838
9. Das M, Djahanbakhch O, Hacıhanefioglu B, Saridogan E, Ikram M, Ghali L, Raveendran M, Storey A. Granulosa cell survival and proliferation are altered in polycystic ovary syndrome. *The Journal of clinical endocrinology and metabolism* 2008; 93:881-887
10. Onalan G, Selam B, Baran Y, Cincik M, Onalan R, Gunduz U, Ural AU, Pabuccu R. Serum and follicular fluid levels of soluble Fas, soluble Fas ligand and apoptosis of luteinized granulosa cells in PCOS patients undergoing IVF. *Hum Reprod* 2005; 20:2391-2395
11. Suzuki HI, Yamagata K, Sugimoto K, Iwamoto T, Kato S, Miyazono K. Modulation of microRNA processing by p53. *Nature* 2009; 460:529-533
12. Vaira V, Verdelli C, Forno I, Corbetta S. MicroRNAs in parathyroid physiopathology. *Molecular and cellular endocrinology* 2016;
13. Hemmatzadeh M, Mohammadi H, Karimi M, Musavishenas MH, Baradaran B. Differential role of microRNAs in the pathogenesis and treatment of Esophageal cancer. *Biomedicine & pharmacotherapy = Biomedecine & pharmacotherapie* 2016; 82:509-519
14. Toll A, Salgado R, Espinet B, Diaz-Lagares A, Hernandez-Ruiz E, Andrades E, Sandoval J, Esteller M, Pujol RM, Hernandez-Munoz I. MiR-204 silencing in intraepithelial to invasive cutaneous squamous cell carcinoma progression. *Molecular cancer* 2016; 15:53
15. Murri M, Insenser M, Fernandez-Duran E, San-Millan JL, Escobar-Morreale HF. Effects of polycystic ovary syndrome (PCOS), sex hormones, and obesity on circulating miRNA-21,

miRNA-27b, miRNA-103, and miRNA-155 expression. *The Journal of clinical endocrinology and metabolism* 2013; 98:E1835-1844

**16.** Sang Q, Yao Z, Wang H, Feng R, Wang H, Zhao X, Xing Q, Jin L, He L, Wu L, Wang L. Identification of microRNAs in human follicular fluid: characterization of microRNAs that govern steroidogenesis in vitro and are associated with polycystic ovary syndrome in vivo. *The Journal of clinical endocrinology and metabolism* 2013; 98:3068-3079

**17.** McCallie B, Schoolcraft WB, Katz-Jaffe MG. Aberration of blastocyst microRNA expression is associated with human infertility. *Fertil Steril* 2010; 93:2374-2382

**18.** Roth LW, McCallie B, Alvero R, Schoolcraft WB, Minjarez D, Katz-Jaffe MG. Altered microRNA and gene expression in the follicular fluid of women with polycystic ovary syndrome. *Journal of assisted reproduction and genetics* 2014; 31:355-362

**19.** Andersen CY, Elbaek HO, Alsbjerg B, Laursen RJ, Povlsen BB, Thomsen L, Humaidan P. Daily low-dose hCG stimulation during the luteal phase combined with GnRHa triggered IVF cycles without exogenous progesterone: a proof of concept trial. *Hum Reprod* 2015; 30:2387-2395

**20.** Rotterdam EA-SPCWG. Revised 2003 consensus on diagnostic criteria and long-term health risks related to polycystic ovary syndrome. *Fertil Steril* 2004; 81:19-25

**21.** Nishi Y, Yanase T, Mu Y, Oba K, Ichino I, Saito M, Nomura M, Mukasa C, Okabe T, Goto K, Takayanagi R, Kashimura Y, Haji M, Nawata H. Establishment and characterization of a steroidogenic human granulosa-like tumor cell line, KGN, that expresses functional follicle-stimulating hormone receptor. *Endocrinology* 2001; 142:437-445

**22.** Wang L, Li H, Yang S, Ma W, Liu M, Guo S, Zhan J, Zhang H, Tsang SY, Zhang Z, Wang Z, Li X, Guo YD, Li X. Cyanidin-3-o-glucoside directly binds to ERalpha36 and inhibits EGFR-positive triple-negative breast cancer. *Oncotarget* 2016;

**23.** Xu S, Linher-Melville K, Yang BB, Wu D, Li J. Micro-RNA378 (miR-378) regulates ovarian estradiol production by targeting aromatase. *Endocrinology* 2011; 152:3941-3951

**24.** Dai A, Sun H, Fang T, Zhang Q, Wu S, Jiang Y, Ding L, Yan G, Hu Y. MicroRNA-133b stimulates ovarian estradiol synthesis by targeting Foxl2. *FEBS letters* 2013; 587:2474-2482

**25.** Yin M, Lu M, Yao G, Tian H, Lian J, Liu L, Liang M, Wang Y, Sun F. Transactivation of microRNA-383 by steroidogenic factor-1 promotes estradiol release from mouse ovarian granulosa cells by targeting RBMS1. *Molecular endocrinology* 2012; 26:1129-1143

**26.** Nie MY, Yu S, Peng S, Fang Y, Wang HM, Yang XK. miR-23a and miR-27a Promote Human Granulosa Cell Apoptosis by Targeting SMAD5. *Biol Reprod* 2015; 93

**27.** Kaur S, Archer KJ, Devi MG, Kriplani A, Strauss JF, Singh R. Differential Gene Expression in Granulosa Cells from Polycystic Ovary Syndrome Patients with and without Insulin Resistance: Identification of Susceptibility Gene Sets through Network Analysis. *J Clin Endocr Metab* 2012; 97:E2016-E2021

28. Jiang L, Huang J, Li L, Chen Y, Chen X, Zhao X, Yang D. MicroRNA-93 promotes ovarian granulosa cells proliferation through targeting CDKN1A in polycystic ovarian syndrome. *The Journal of clinical endocrinology and metabolism* 2015; 100:E729-738
29. Xiang YG, Song YX, Li Y, Zhao DM, Ma LY, Tan L. miR-483 is Down-Regulated in Polycystic Ovarian Syndrome and Inhibits KGN Cell Proliferation via Targeting Insulin-Like Growth Factor 1 (IGF1). *Med Sci Monitor* 2016; 22:3383-3393
30. Musto A, Navarra A, Vocca A, Gargiulo A, Minopoli G, Romano S, Romano MF, Russo T, Parisi S. miR-23a, miR-24 and miR-27a protect differentiating ESCs from BMP4-induced apoptosis. *Cell death and differentiation* 2015; 22:1047-1057
31. Tian Y, Fu S, Qiu GB, Xu ZM, Liu N, Zhang XW, Chen S, Wang Y, Sun KL, Fu WN. MicroRNA-27a promotes proliferation and suppresses apoptosis by targeting PLK2 in laryngeal carcinoma. *Bmc Cancer* 2014; 14
32. Sabirzhanov B, Zhao ZR, Stoica BA, Loane DJ, Wu JF, Borroto C, Dorsey SG, Faden AI. Downregulation of miR-23a and miR-27a following Experimental Traumatic Brain Injury Induces Neuronal Cell Death through Activation of Proapoptotic Bcl-2 Proteins. *J Neurosci* 2014; 34:10055-10071
33. Zhou L, Liang X, Zhang LL, Yang LY, Nagao N, Wu HK, Liu C, Lin SC, Cai GX, Liu JW. MiR-27a-3p functions as an oncogene in gastric cancer by targeting BTG2. *Oncotarget* 2016; 7:51943-51954
34. Wan XC, Huang WH, Yang S, Zhang YL, Zhang P, Kong Z, Li T, Wu H, Jing FX, Li Y. Androgen-induced miR-27A acted as a tumor suppressor by targeting MAP2K4 and mediated prostate cancer progression. *Int J Biochem Cell B* 2016; 79:249-260
35. Tilly JL. Apoptosis and ovarian function. *Reviews of reproduction* 1996; 1:162-172
36. Morita Y, Tilly JL. Oocyte apoptosis: Like sand through an hourglass. *Dev Biol* 1999; 213:1-17
37. Mansouri-Attia N, Tripurani SK, Gokul N, Piard H, Anderson ML, Eldin K, Pangas SA. TGFbeta signaling promotes juvenile granulosa cell tumorigenesis by suppressing apoptosis. *Molecular endocrinology* 2014; 28:1887-1898
38. Wu S, Lin Y, Xu D, Chen J, Shu M, Zhou Y, Zhu W, Su X, Zhou Y, Qiu P, Yan G. MiR-135a functions as a selective killer of malignant glioma. *Oncogene* 2012; 31:3866-3874
39. Dewailly D, Robin G, Peigne M, Decanter C, Pigny P, Catteau-Jonard S. Interactions between androgens, FSH, anti-Mullerian hormone and estradiol during folliculogenesis in the human normal and polycystic ovary. *Hum Reprod Update* 2016; 22:709-724
40. Li Y, Fang Y, Liu Y, Yang X. MicroRNAs in ovarian function and disorders. *Journal of ovarian research* 2015; 8:51
41. Guo Y, Sun J, Lai D. Role of microRNAs in premature ovarian insufficiency. *Reproductive biology and endocrinology : RB&E* 2017; 15:38

42. Ni XR, Sun ZJ, Hu GH, Wang RH. High Concentration of Insulin Promotes Apoptosis of Primary Cultured Rat Ovarian Granulosa Cells Via Its Increase in Extracellular HMGB1. *Reprod Sci* 2015; 22:271-277
43. Catteau-Jonard S, Dewailly D. Pathophysiology of polycystic ovary syndrome: the role of hyperandrogenism. *Frontiers of hormone research* 2013; 40:22-27
44. Cedars MI, Steingold KA, de Ziegler D, Lapolt PS, Chang RJ, Judd HL. Long-term administration of gonadotropin-releasing hormone agonist and dexamethasone: assessment of the adrenal role in ovarian dysfunction. *Fertil Steril* 1992; 57:495-500
45. Sen A, Prizant H, Light A, Biswas A, Hayes E, Lee HJ, Barad D, Gleicher N, Hammes SR. Androgens regulate ovarian follicular development by increasing follicle stimulating hormone receptor and microRNA-125b expression. *Proceedings of the National Academy of Sciences of the United States of America* 2014; 111:3008-3013
46. Fletcher CE, Dart DA, Sita-Lumsden A, Cheng H, Rennie PS, Bevan CL. Androgen-regulated processing of the oncomir MiR-27a, which targets Prohibitin in prostate cancer. *Hum Mol Genet* 2012; 21:3112-3127

**Figure 1 (black and white) Expression of miR-27a-3p and other miRNAs in human GCs of non-treated and treated PCOS and normal healthy patients.** (A-H) The expression of miR-27a-3p, miR-27a-5p, miR-23a, and miR-24-2 in excised GCs of 12 healthy control and 21 PCOS patients undergoing IVF treatment and 13 non-PCOS cuneiform ovarian resections and non-treated 17 PCOS. MiR-27a-3p expression in GCs (A) and ovaries (B) in the PCOS group compared with the control group. MiR-27a-5p (C, D), miR-23a (E, F), miR-24-2 (G, H) expression in the both groups. PCOS OV, PCOS ovarian. \*,  $P < 0.05$ ; \*\*,  $P < 0.01$

**Figure 2 (black and white) Effects of insulin treatment on miR-27a-3p in KGN cells.** (A) The expression of miR-27a-3p in KGN cells with different amounts of insulin. KGN cells were stimulated for 24 h without (0) or with 1, 10, and 100 ng/mL of insulin. (B) The predicted binding sites of STAT1 and STAT3 by JASPAR software in the 2000 nucleotides upstream of the miR-27a-3p. (C) The relative expression level of miR-27a-3p in STAT1-overexpressed cells and controls. (D-F) Protein levels (D) and quantification of STAT1 (E) and STAT3 (F) in insulin-treated KGN cells. \*,  $P < 0.05$ ; \*\*,  $P < 0.01$

**Figure 3 (black and white) Effects of miR-27a-3p on cell proliferation and apoptosis in KGN cells.** (A) The expression levels of miR-27a-3p in KGN cells after transfection with the miR-27a-3p mimic. (B) Cell viability of KGN cells. (C) Apoptosis rate of KGN cells. (D) Quantification of cell cycle (the rate of G0/G1 and G2/M). (E) The protein levels of PCNA in KGN cells. (F) Expression of cell cycle-related genes (CDK6, cyclin D1, and cyclin E) in KGN cells. (G) Luciferase activity of SMAD5 gene 3'-UTR. (H) The mRNA level of SMAD5 in KGN cells. (I) The protein level of SMAD5 in KGN cells. (J-K) The mRNA expression level of SMAD5 in primary PCOS GCs (J) and OV (K). (L) The mRNA expression level of SMAD5 in

PCOS GCs from public database. GAPDH was used to normalize the expression level. \*,  $P < 0.05$ ; \*\*,  $P < 0.01$ .

**Figure 4 (black and white) Effects of knockdown/ overexpression of SMAD5 on KGN cells.**

(A, B) The mRNA (A) and protein (B) levels of SMAD5 in KGN cells after si-SMAD5 transfection. (C) Cell viability of KGN cells after si-SMAD5 transfection. (D) Apoptosis rate of KGN cells after si-SMAD5 transfection. (E, F) The mRNA (E) and protein (F) levels of SMAD5 in KGN cells after pSMAD5 transfection. (G) Cell viability of KGN cells after pSMAD5 transfection. (H) Apoptosis rate of KGN cells after pSMAD5 transfection. \*,  $P < 0.05$ ; \*\*,  $P < 0.01$

**Figure 5 (black and white) Effects of insulin treatment on apoptosis and SMAD5**

**expression in KGN cells.** (A) Cell viability of KGN cells treated with 100 ng/mL of insulin for 48 h. (B) Quantification of the apoptotic effect in KGN cells treated with insulin for 48 h. (C) Effects of 100 ng/mL insulin 48 h treatment on SMAD5 protein expression in KGN cells. (D) The relative expression levels of SMAD5 protein were normalized to GAPDH. \*,  $P < 0.05$ ; \*\*,  $P < 0.01$

**Figure 6 (black and white) Expression of miR-27a-3p in primary GCs treated with insulin.**

The expression level of miR-27a-3p in GCs from PCOS and normal healthy patients treated with different doses of insulin. \*,  $P < 0.05$ ; \*\*,  $P < 0.01$

Table 1 Characteristics of the subjects in the study

Table 1 Characteristics of the subjects in the paper.

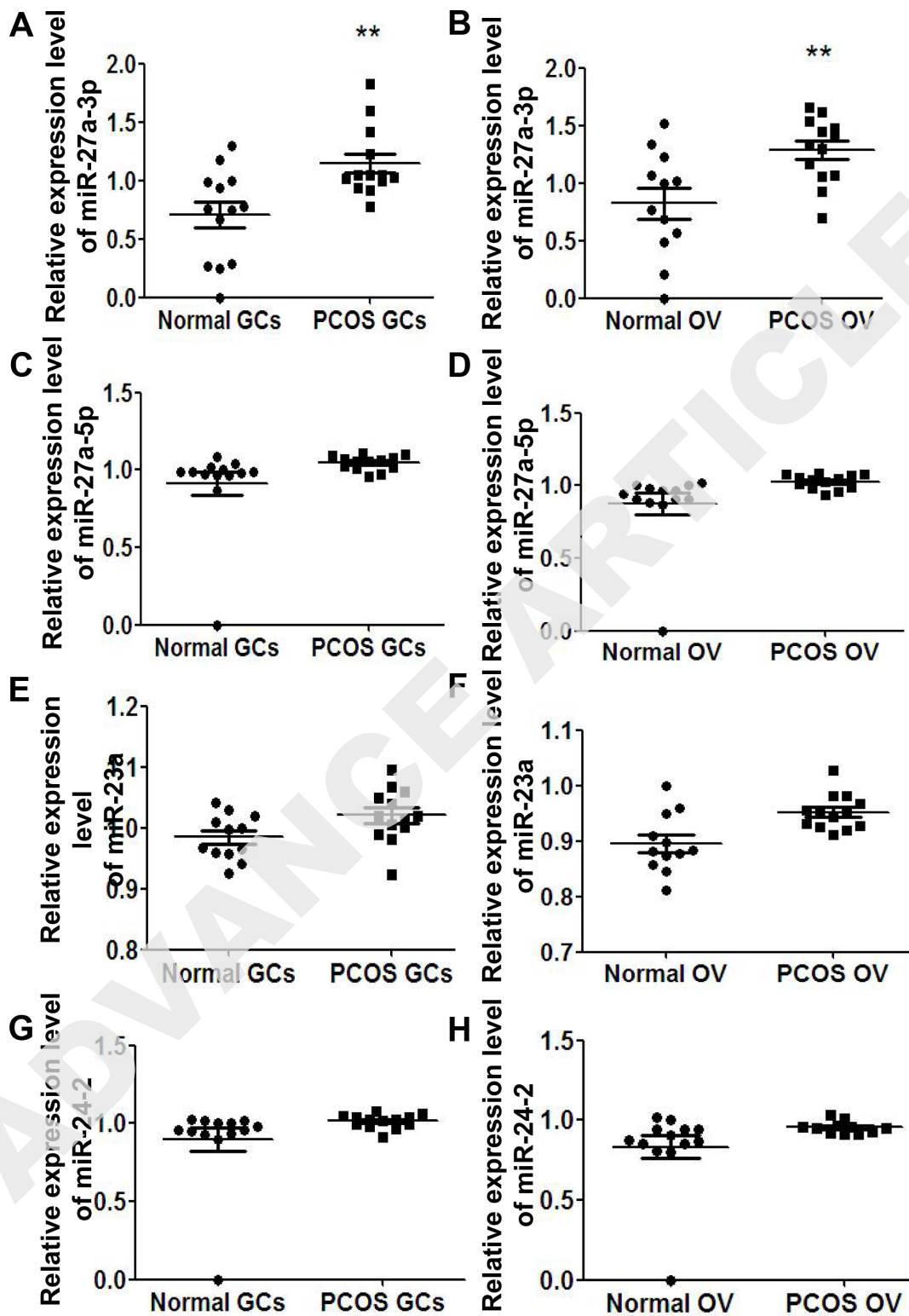
	Control group (n=13)	PCOS group (n=21)	P value
Age (years)	30.00 ± 0.74 [2.77]	28.67 ± 0.675 [3.698]	0.24
BMI (kg/m <sup>2</sup> )	23.63 ± 1.701	24.69 ± 1.193	0.5670
Testosterone [nmol/L]	1.30 ± 0.15 [0.57]	1.95 ± 0.13 [0.63]	0.0036
FAI	2.16 ± 0.39 [1.46]	3.88 ± 0.61 [2.77]	0.04
Glucose [mmol/L]	4.52 ± 0.2 [0.75]	4.59 ± 0.16 [0.63]	0.77
Insulin [μU/mL]	4.22 ± 0.28 [1.03]	8.53 ± 1.12 [4.86]	0.0028
HOMA	0.84 ± 0.06 [0.22]	1.77 ± 0.25 [1.08]	0.0034
SHBG [nmol/L]	83.39 ± 12.79 [47.85]	75.64 ± 10.51 [49.31]	0.64
DHEA-S [μmol/L]	6.43 ± 0.52 [1.94]	7.92 ± 0.52 [2.46]	0.06
Hyperandrogenism, (n)%	4 (28.6%)	15 (65.2%)	
Normal androgen, (n)%	10 (71.4%)	8 (34.8%)	

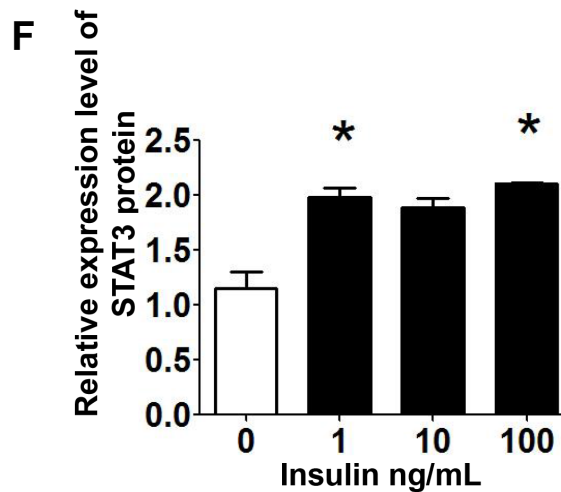
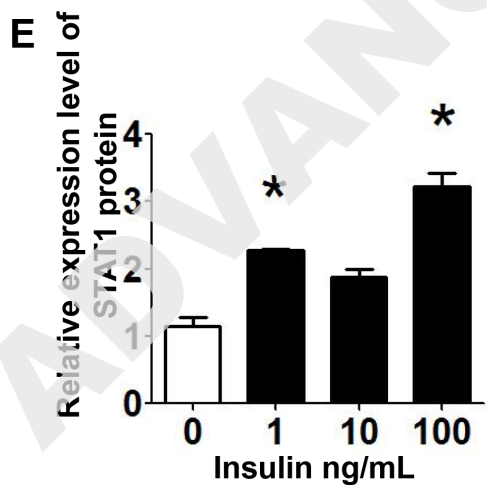
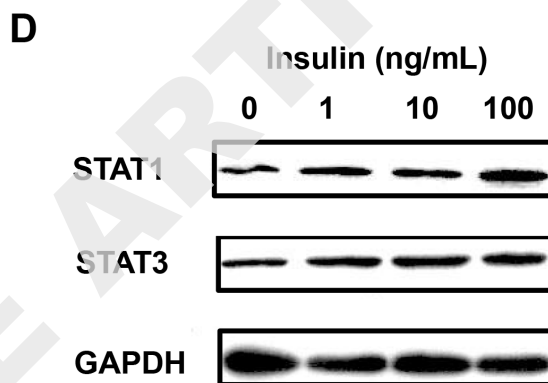
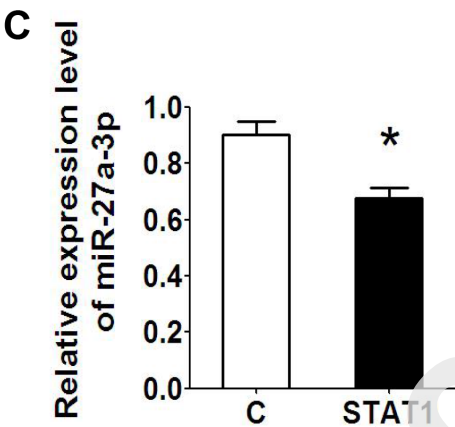
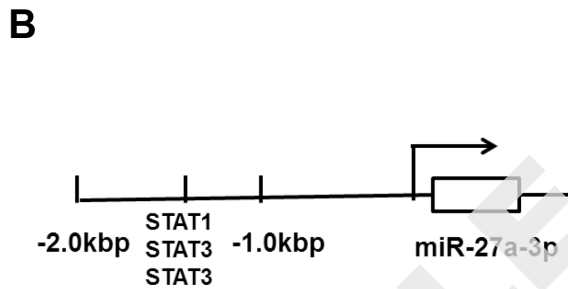
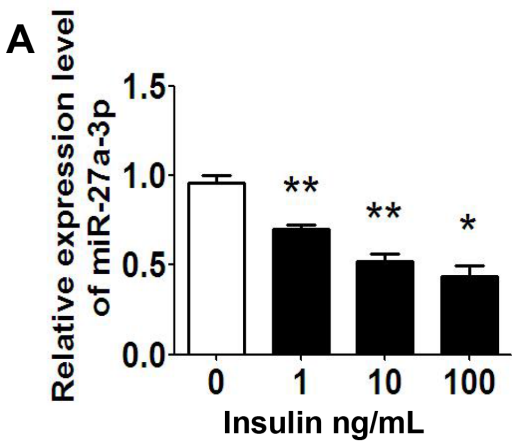
Abbreviation: BMI, Body Mass Index; FAI, Free Androgen Index; SHBG, Sex Hormone-Binding Globulin; DHEA-S, Dehydroepiandrosterone Sulfate; HOMA, Homeostasis Model Assessment.

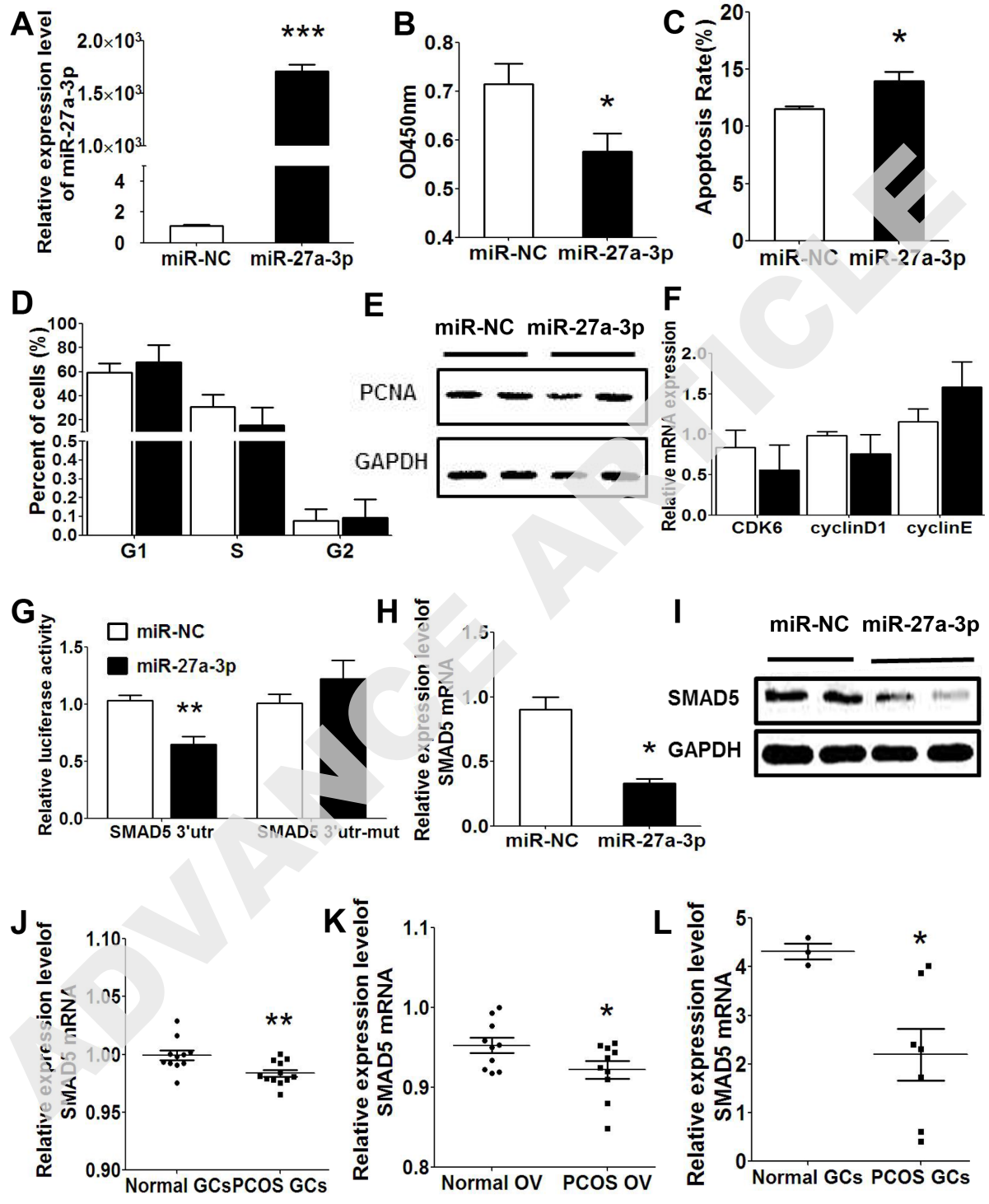
Data are presented as Mean ± SEM [SD]

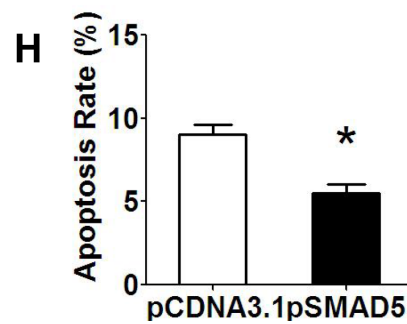
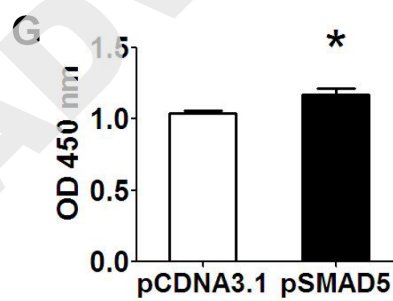
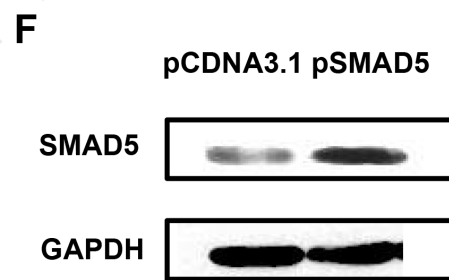
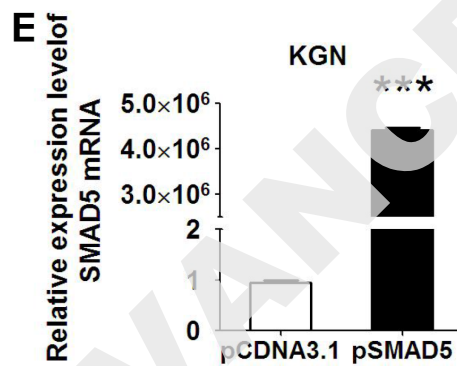
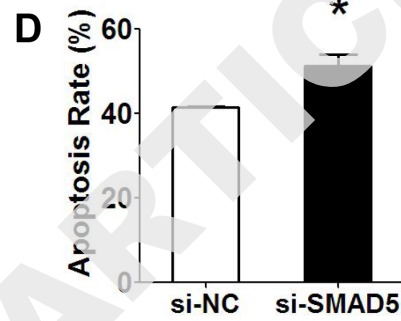
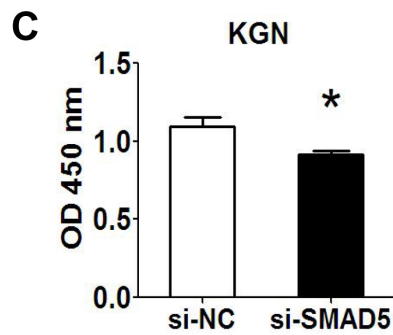
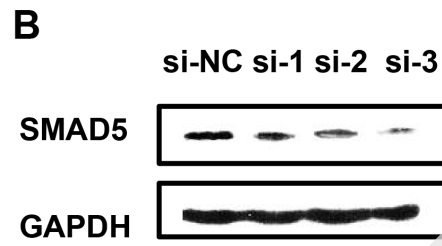
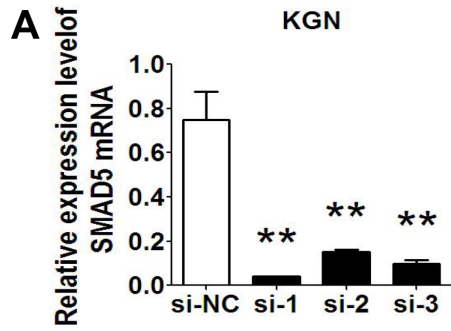
Peptide/protein target	Antigen sequence (if known)	Name of Antibody	Manufacturer, catalog #, and/or name of individual providing the antibody	Species raised in; monoclonal or polyclonal	Dilution used	RRID (required in revised MSs)
SMAD5		SMAD5 Antibody	CST #9517S	Rabbit; polyclonal	1/1000	AB_10699149
PCNA		PCNA (PC10)	Santa Cruz Biotechnology sc-56	Mouse monoclonal	1/1000	AB_628110
GAPDH		GAPDH (14C10)	CST #2118	Rabbit; monoclonal	1/1000	AB_561053
STAT1		P84/P91 (E-23)	Santa Cruz Biotechnology sc-346	Rabbit; polyclonal	1/1000	AB_632435
STAT3		124H6	CST #9139s	Mouse; monoclonal	1/1000	AB_10694804

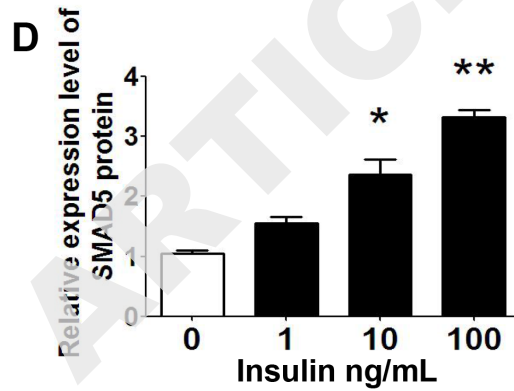
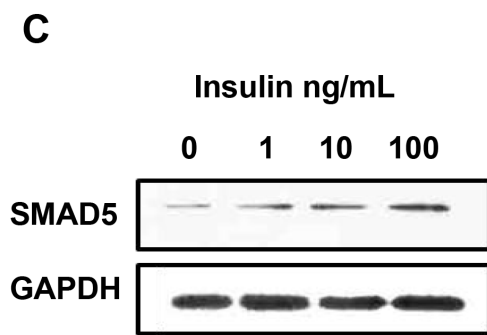
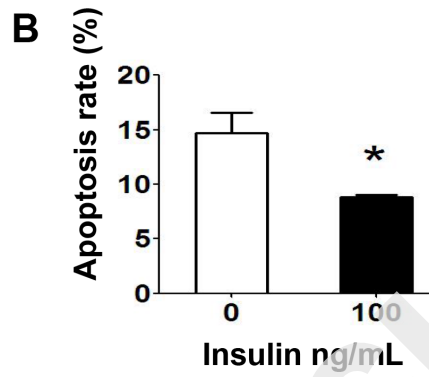
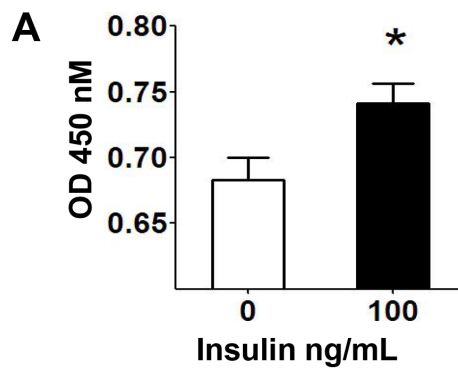




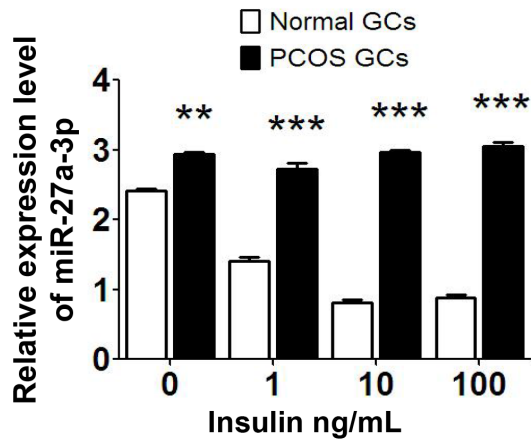












ADVANCE ARTICLE